JOURNAL OF BACTERIOLOGY, Jan. 1998, p. 73–82 Vol. 180, No. 1
0021-9193/98/$04.00+0


# RimM and RbfA Are Essential for Efficient Processing of 16S rRNA in *Escherichia coli*

GÖRAN O. BYLUND, L. CHARLOTTA WIPEMO, L. A. CARINA LUNDBERG, AND P. MIKAEL WIKSTRÖM*

*Department of Microbiology, Umeå University, S-901 87 Umeå, Sweden*

Received 11 August 1997/Accepted 28 October 1997

**The *trmD* operon is located at 56.7 min on the genetic map of the *Escherichia coli* chromosome and contains the genes for ribosomal protein (r-protein) S16, a 21-kDa protein (RimM, formerly called 21K), the tRNA ($m^1$G37)methyltransferase (TrmD), and r-protein L19, in that order. Previously, we have shown that strains from which the *rimM* gene has been deleted have a sevenfold-reduced growth rate and a reduced translational efficiency. The slow growth and translational deficiency were found to be partly suppressed by mutations in *rpsM*, which encodes r-protein S13. Further, the RimM protein was shown to have affinity for free ribosomal 30S subunits but not for 30S subunits in the 70S ribosomes. Here we have isolated several new suppressor mutations, most of which seem to be located close to or within the *nusA* operon at 68.9 min on the chromosome. For at least one of these mutations, increased expression of the ribosome binding factor RbfA is responsible for the suppression of the slow growth and translational deficiency of a Δ*rimM* mutant. Further, the RimM and RbfA proteins were found to be essential for efficient processing of 16S rRNA.**

The *trmD* operon, located at min 56.7 on the molecular genetic map of the *Escherichia coli* chromosome (23), contains the genes for ribosomal protein (r-protein) S16 (*rpsP*), RimM (a 21-kDa protein formerly called 21K) (*rimM*, previously called *21K* and *yfjA*), the tRNA($m^1$G37)methyltransferase (or TrmD) (*trmD*), and r-protein L19 (*rplS*), in that order (8) (Fig. 1). The RimM and TrmD proteins are found in 12- and 40-fold-lower amounts, respectively, than the two r-proteins (47). This difference in expression is due to translational-level regulation (9, 47) by sequestering of the Shine-Dalgarno sequences and start codons of the *rimM* and *trmD* genes in mRNA secondary structures that prevent access of the translational-initiation regions to the ribosomes (48, 50).

All the genes in the *trmD* operon encode proteins that are involved in translation. Strains from which the chromosomal *rpsP* gene copy (for S16) has been deleted are nonviable in the absence of complementing gene copies (33), possibly because S16 is essential for the assembly of the 30S ribosomal subunits (13). Recently, S16 has been found to be an endonuclease also (30). r-protein L19 is essential for the viability of wild-type *E. coli* cells (33); however, compensatory mutations can rescue L19-lacking mutants (33, 42). Also, L19 seems important for ribosome assembly, since a reduction in the synthesis of L19 due to a polar insertion in *rimM* resulted in the accumulation of an assembly intermediate of the 50S ribosomal subunit (33). The tRNA($m^1$G37)methyltransferase modifies the guanosine in position 37 next to the anticodon of a subset of the tRNAs in *E. coli* and *Salmonella typhimurium* (see references 3 and 4), and the modification is important for maintaining the correct reading frame during translation (5, 12). In addition, strains from which the *trmD* gene has been deleted have at least a fivefold-reduced growth rate in rich medium (33). Similarly, strains lacking the RimM protein show a five- to sevenfold-reduced growth rate, depending on the growth medium used (7, 33). Recently, it has been found that mutants lacking the RimM protein show reduced translational efficiency. In agreement with a role in translation, the RimM protein shows affinity for the 30S ribosomal subunits (7). The slow growth and translational deficiency of a Δ*rimM* mutant can be partially suppressed by mutations in *rpsM*, which encodes r-protein S13 (7). In the present study we have isolated and characterized 26 additional suppressor mutations that increase the growth rate of a Δ*rimM* mutant, 23 of which seem to be located within or close to the *nusA* operon at 68.9 min on the chromosome. We demonstrate that at least one of these suppressor mutations increases expression of the ribosome binding factor RbfA (10). Moreover, the Δ*rimM* mutation was suppressed by an increased gene dosage of *rbfA*, suggesting that the mechanism behind the suppression was an increased synthesis of RbfA. Furthermore, mutants lacking either RimM or RbfA showed reduced efficiency in the processing of 16S rRNA, implying that both proteins are important for the maturation of the ribosomal 30S subunits.

## MATERIALS AND METHODS

**Strains, phages, and plasmids.** Strains, phages, and plasmids used are listed in Table 1. Strain GOB162 was constructed by transducing strain MW100 with phage P1 grown on strain CD28 and selecting for $Km^r$.

**Plasmid constructions.** Plasmid pGOB3 was constructed by cloning *Kpn*I-digested chromosomal DNA isolated from strain GOB083 (*sdr-43 truB2422*::mini-Tn*10*Cm) into the low-copy-number vector pCL1921 and selecting for $Cm^r$ conferred by the mini-Tn*10*Cm linked to *sdr-43*. Plasmids pGOB7 and pGOB8 were constructed by digesting pGOB3 with *Bam*HI and *Eco*RI, respectively, and religating (see Fig. 3). To construct pGOB18, a fragment carrying the *rbfA* gene and its tentative promoter was amplified from strain GOB083 by PCR using the oligonucleotides 5′-TTTTGTCGACAGAACTACAACGACGTCC-3′ and 5′-TTTTGGATCCTGAGGTTTATCCAGCAAC-3′ (containing restriction sites for *Sal*I and *Bam*HI, respectively), digested with *Sal*I and *Bam*HI, and cloned into pCL1921. Plasmid pGOB19 was constructed in a similar way except that the *Sal*I site included in the first oligonucleotide was replaced by an *Eco*RI site.

**Media and growth conditions.** The minimal medium used was morpholinepropanesulfonic acid (MOPS) (28) supplemented with 0.4% glucose. Rich medium was either rich MOPS (27) or Luria-Bertani (LB) medium (2) supplemented with medium E plus thiamine (45) and 0.4% glucose. Cultures were grown at 37°C, and the growth was monitored either on a Zeiss PMQ3 spectrophotometer at 420 or 600 nm or on a Klett-Summerson colorimeter equipped with a red filter.

**P1 and λ transduction.** Standard procedures were used for generalized transduction with P1 (24). Transduction of different recipient strains to $Km^r$ by λ439Δ*rimM-2* was carried out mainly as described by Kulakauskas et al. (19).

* Corresponding author. Mailing address: Department of Microbiology, Umeå University, S-901 87 Umeå, Sweden. Phone: 46-90-7856754. Fax: 46-90-772630. E-mail: Mikael.Wikstrom@micro.umu.se.

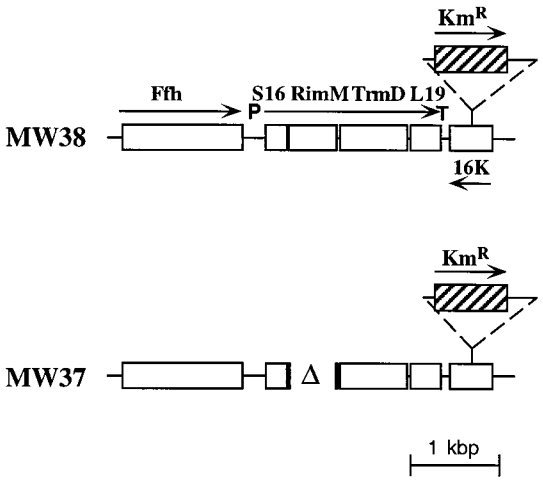


FIG. 1. Genetic organization of the *trmD* operon region of the chromosome of the Δ*rimM-2* mutant MW37 and the congenic *rimM*$^+$ strain MW38. P and T indicate the promoter and terminator, respectively, of the *trmD* operon. The arrows above and below the genes for Ffh (named Ffh for fifty-four homolog of the 54-kDa protein of the signal recognition particle) and a 16-kDa protein designated 16K, respectively, show the orientations of the transcripts and not their actual sizes. The Km$^r$ gene derived from transposon Tn*903* was previously inserted into the gene for the nonessential 16K protein (33).

**Construction of Tn*10* libraries.** Libraries of mini-Tn*10*Cm insertions were constructed as described elsewhere by using λNK1324 (17).

**PCR amplification of chromosomal DNA and DNA sequencing.** Regions of the *E. coli* chromosome were amplified from colonies resuspended in $H_2O$ by PCR (26, 37). *Pfu* DNA polymerase from Stratagene (La Jolla, Calif.) was used if the fragments obtained were to be cloned into plasmids, and *Taq* DNA polymerase from Boehringer Mannheim Scandinavia AB (Bromma, Sweden) was used in all other cases. Fragments obtained were separated on agarose gels, cut out, and purified with Gene Clean from Bio 101 Inc. (La Jolla, Calif.). DNA sequencing of PCR fragments was carried out with Thermo Sequenase as described by Amersham Life Science, Inc. (Cleveland, Ohio), whereas plasmid DNA sequencing was carried out with a T7 sequencing kit purchased from Pharmacia Biotech (Uppsala, Sweden).

**Determination of polypeptide chain growth rate.** The polypeptide chain growth rate ($cgr_p$) of β-galactosidase was determined by measuring the time necessary for the first β-galactosidase activity to appear after induction (the delay time) with 0.5 mM isopropyl-β-D-thiogalactopyranoside (IPTG) essentially as described by Schleif et al. (40). Cells were grown in MOPS medium to an optical density at 420 nm of 0.5, at which point IPTG was added. Samples (0.5 ml) were withdrawn at intervals of 5 or 10 s and transferred to tubes on ice containing 0.5 ml of Z buffer (24) supplemented with 200 μg of chloramphenicol/ml, 0.005% sodium dodecyl sulfate, and 50 μl of chloroform. The β-galactosidase activity in the samples was determined according to the method of Miller (24).

**Northern blot analysis.** Total RNA was prepared according to the work of von Gabain et al. (46) and subjected to Northern blot analysis mainly as described by Sambrook et al. (38). Equal amounts of the RNA from the different strains were loaded onto Northern gels as determined both by spectrophotometric measurements at 260 nm and by ethidium bromide staining of aliquots of the RNA electrophoresed on agarose gels. DNA fragments used as probes were purified as described above and labeled with [α-$^{32}$P]dATP by using the Megaprime DNA labeling system from Amersham Life Science, Inc.

**Analysis of proteins by 2D gel electrophoresis.** Steady-state cultures of bacterial cells were grown at 37°C to an optical density at 600 nm of 0.25 and then shifted to 15°C. Just prior to the shift, 1-ml aliquots of the cultures were labeled for 15 min with 250 μCi of [$^{35}$S]methionine each (>1,000 Ci/mmol) and chased with 0.167 ml of 0.2 M methionine for 3 min. Similarly, 1-ml aliquots withdrawn 30 min after the temperature shift were labeled for 30 min and chased for 6 min. Extracts were prepared mainly as described previously (44). O'Farrell two-dimensional (2D) polyacrylamide gels (31) were used to analyze the protein expression pattern. One million counts per minute was loaded onto each first-dimension isoelectric focusing gel containing ampholines 3 to 10 and Duracryl acrylamide from Oxford Glycosystems. The first dimension was run as described by Millipore Intertech (Bedford, Mass.), whereas the second dimension was 10 to 17.5% gradient polyacrylamide slab gels containing sodium dodecyl sulfate. The gels were dried and exposed to X-ray film, and the autoradiographs obtained were analyzed by the Bio Image 2-D Analyzer, version 6.0.3, from B.I. Systems Corporation.

TABLE 1. Bacterial strains, bacteriophages, and plasmids

| Strain, phage, or plasmid | Genotype | Source or reference[a] |
|---|---|---|
| Strains | | |
| ORN103 | *thr-1 leuB thi-1* Δ*(argF-lac)U169 malA1 xyl-7 ara-13 mtl-2 gal-6 rpsL tonA2 minA minB recA13* Δ*pil* | 32 |
| CD28 | F$^-$ *ara* Δ*(gpt-lac)5 rbfA*::*kan* | 10 |
| GOB007 | Hfr P4X Δ*rimM-2 16K*::*nptI sdr-43 truB2422*::mini-Tn*10*Cm | |
| GOB083 | Hfr P4X *sdr*-43 truB2422::mini-Tn*10*Cm | |
| GOB113 | Hfr P4X *sdr*$^+$ truB2422::mini-Tn*10*Cm | |
| GOB162 | Hfr P4X *rbfA*::*kan* | |
| MW37 | Hfr P4X Δ*rimM-2 16K*::*nptI* | 33 |
| MW38 | Hfr P4X *16K*::*nptI* | 33 |
| MW100 | Hfr P4X | 49 |
| PW098 | Hfr P4X Δ*rimM-2 16K*::*nptI sdr-32* | |
| PW100 | Hfr P4X Δ*rimM-2 16K*::*nptI sdr-34* | |
| PW101 | Hfr P4X Δ*rimM-2 16K*::*nptI sdr-35* | |
| PW105 | Hfr P4X Δ*rimM-2 16K*::*nptI sdr-39* | |
| PW107 | Hfr P4X Δ*rimM-2 16K*::*nptI sdr-41* | |
| PW109 | Hfr P4X Δ*rimM-2 16K*::*nptI sdr-43* | |
| PW119 | Hfr P4X Δ*rimM-2 16K*::*nptI sdr-53* | |
| PW121 | Hfr P4X Δ*rimM-2 16K*::*nptI sdr-55* | |
| Bacteriophages | | |
| λ439/λ22D7 | *rimM*$^+$ | 18 |
| λ439Δ*rimM-2* | Δ*rimM-2 16K*::*nptI* | 33 |
| P1*vir* | | Laboratory stock |
| Plasmids | | |
| pCL1921 | Str$^r$ Spc$^r$ | 20 |
| pGOB3 | pCL1921-′*infB rbfA*$^+$ *truB2422*::mini-Tn*10*Cm *rpsO*$^+$ *pnp*$^+$ | |
| pGOB7 | pCL1921-′*truB rpsO*$^+$ *pnp*$^+$ | |
| pGOB8 | pCL1921-′*infB rbfA*$^+$ *truB2422*::mini-Tn*10*Cm’ | |
| pGOB18 | pCL1921-′*infB rbfA*$^+$ | |
| pGOB19 | pCL1921-′*infB rbfA*$^+$ | |
| pGOB22 | pCL1921-′*infB rbfA*$^+$ | |

[a] Unless otherwise noted, the source was this study.

**Expression of *rbfA* in minicells.** The minicell-producing strain AA10 was transformed with plasmid pGOB18 containing the *rbfA* gene. Preparation and labeling of plasmid-containing minicells were carried out essentially as described previously (16, 43).

**Primer extension on rRNA.** Total RNA was prepared either with the Total RNA Kit from Qiagen GmbH (Hilden, Germany) or according to the work of von Gabain et al. (46). Two micrograms of the RNA was subjected to primer extension with 2 pmol of a $^{32}$P-end-labeled primer specific for 5S rRNA (5′-GGCGTTTCACTTCTGAG-3′), 16S rRNA (5′-CGACTTGCATGTGTTAGG-3′), or 23S rRNA (5′-CGTCCTTCATCGCCTCTG-3′) by using avian myeloblastosis virus reverse transcriptase from Pharmacia Biotech (Sollentuna, Sweden). Small aliquots of the reaction mixtures (1:100 to 1:500) were run next to a DNA sequencing ladder on 6% polyacrylamide gels containing 8 M urea. The gels were dried and exposed to Hyperfilm-MP from Amersham International plc (Buckinghamshire, England). The autoradiographs obtained were scanned with a ScanMaker III from Microtek International, Inc., and processed with Adobe Photoshop 3.0. The gels were also exposed to a phosphor screen, and the amounts of radioactivity in the primer extension products were quantified by using ImageQuant from Molecular Dynamics, Inc.

## RESULTS

**New suppressor mutations increase the growth rate of the Δ*rimM-2* mutant up to fourfold.** The growth rate of the Δ*rimM-2* mutant MW37 is 4.4-fold lower in LB medium and 7-fold lower in MOPS minimal medium containing 0.4% glu-

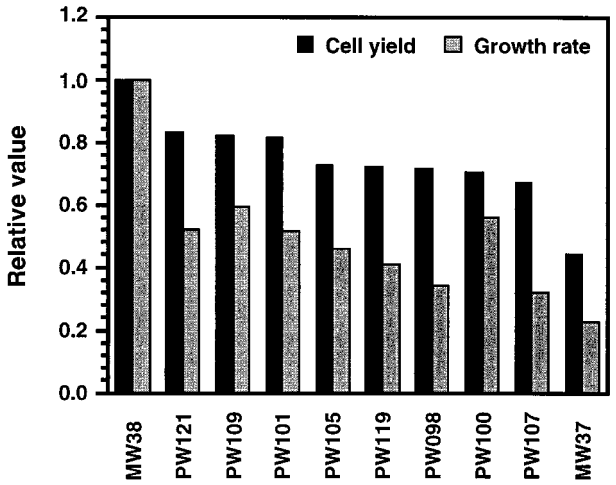


FIG. 2. Relative cell yields and growth rates for wild-type and mutant strains. The cell yields for the different strains grown in MOPS minimal medium were calculated as $\Delta A_{420}/\Delta$(glucose concentration, expressed as a percentage). The glucose concentrations used were 0.005 to 0.1%. The growth rates are for growth in LB medium. Both the cell yield values and the growth rates have been normalized to those for strain MW38.

cose than that of the congenic *rimM*$^+$ strain MW38 (7). In an attempt to isolate mutations that suppressed the slow growth of strain MW37, 19 single colonies of strain MW37 were grown in LB overnight at 37°C, reinoculated from the overnight cultures into fresh medium, and incubated again. This procedure was repeated for 3 to 5 days, and samples were withdrawn from each overnight culture and streaked onto rich-medium plates to examine if any faster-growing derivatives had arisen. In this way, 29 independent suppressor-containing mutants (PW093 to PW121) were isolated; from some of the original cultures, more than one class of mutants was obtained, as judged by differences in their growth rates. That the isolated clones indeed were derivatives of the Δ*rimM-2* mutant was confirmed by PCR analysis using primers specific for the DNA sequences flanking the deletion (data not shown). Three of the mutations were shown to be in *rpsM*, encoding r-protein S13, as presented in a separate report (7).

To quantify the efficiency of the suppressor mutations, the steady-state growth rate in rich medium was determined for 28 of the isolated suppressor-containing clones. The strongest suppressor mutation, *sdr-43* (named *sdr* for suppressor of deletion of *rimM*), increased the growth rate 2.6-fold (strain PW109), resulting in a growth rate which was 60% of that of the *rimM*$^+$ strain MW38, while the weakest suppressor, *sdr-41* (strain PW107), increased the growth rate 1.4-fold (Fig. 2). Further, the growth rate of strain PW109 in MOPS minimal medium containing 0.4% glucose was fourfold higher than that of strain MW37 (data not shown).

**The suppressor mutations improve the energy utilization efficiency and translational-elongation rate of the Δ*rimM-2* mutant.** Previously, we have shown that strains lacking RimM seem to have reduced energy utilization efficiency, as demonstrated by a lower stationary-phase cell density at a given concentration of carbon source in the growth medium, and that mutations in *rpsM*, coding for r-protein S13, suppress this deficiency (7). To see if some of the other suppressor mutations isolated here also altered the energy utilization efficiency, the stationary-phase cell density was determined for eight of the suppressor strains grown in MOPS minimal medium containing different amounts of glucose (Fig. 2). All of them had a higher ratio of cell yield to carbon source concentration than the suppressor-free strain MW37, suggesting that the new suppressor mutations increased the energy utilization efficiency. Since translation is the single most energy-consuming process in the cell, these results suggested that the suppressor mutations increased the translational proficiency of the Δ*rimM-2* mutant. To test this, we measured the $cgr_p$ of β-galactosidase for two of the Δ*rimM-2*-containing suppressor strains. As shown in Table 2, strains PW098 (Δ*rimM-2 sdr-32*) and PW109 (Δ*rimM-2 sdr-43*) had a higher $cgr_p$ of β-galactosidase than did strain MW37 (Δ*rimM-2*). In conclusion, at least two of the mutations isolated here as suppressors of the slow growth of the Δ*rimM-2* strain MW37 suppressed the translational deficiency of the Δ*rimM-2* mutant.

TABLE 2. β-Galactosidase $cgr_p$'s of mutant and wild-type strains

| Strain | Relevant marker(s) | $cgr_p$ (no. of amino acids per s)[a] |
|---|---|---|
| MW38 | *rimM*$^+$ | 12.0 (11.1–12.8) |
| MW37 | Δ*rimM-2* | 8.6 (8.5–8.7) |
| PW098 | Δ*rimM-2 sdr-32* | 10.4 (9.7–11.1) |
| PW109 | Δ*rimM-2 sdr-43* | 10.9 (10.7–11.1) |

[a] The $cgr_p$ of β-galactosidase in MOPS minimal medium supplemented with 0.4% glucose was measured as described by Schleif et al. (40).

**The slow growth of the Δ*rimM-2* mutant MW37 is suppressed by increased gene dosage of *rbfA*.** In order to localize one of the suppressor mutations, a library of mini-Tn*10*Cm insertions was constructed on the *sdr-43*-containing strain PW109 and several clones with a mini-Tn*10*Cm linked to *sdr-43* were identified by transducing strain MW37 (Δ*rimM-2*) with phage P1 grown on the library, selecting for Cm$^r$, and screening for growth faster than that of strain MW37. One clone that had a mini-Tn*10*Cm 95% linked to *sdr-43*, as demonstrated by backcrosses to MW37, was used in further studies (strain GOB007). The cotransduction frequency implied that *sdr-43* was approximately 1.6 kb from the mini-Tn*10*Cm. Therefore, the mini-Tn*10*Cm was cloned together with the flanking chromosomal DNA into the low-copy-number vector pCL1921, selecting for Cm$^r$. The resultant clone, pGOB3, was shown by DNA sequencing to contain genes from the 68.9-min region of the chromosome. The sequence immediately upstream from the mini-Tn*10*Cm corresponded to codon 170 of *truB* (Fig. 3), and the insertion is hereafter designated *truB2422*::mini-Tn*10*Cm. Plasmid pGOB3 was found to suppress the slow growth of the Δ*rimM-2* mutant (Fig. 3). By subcloning, it appeared that the *rbfA* gene (encoding ribosome binding factor A) just upstream of *truB* was responsible for the observed suppression (pGOB8). The *rbfA* gene is the fifth gene in the polycistronic *nusA* operon, starting with the *metY* gene, and has been suggested to be expressed from an internal promoter located 170 bp upstream of *rbfA* (39). The region containing *rbfA* and its tentative promoter was PCR amplified from strain GOB083 (*sdr-43 truB2422*::mini-Tn*10*Cm) and cloned into the low-copy-number vector pCL1921. The resultant plasmid clone, pGOB18, with *rbfA* in the same orientation as the *lac* promoter of the vector, suppressed the slow growth of the Δ*rimM-2* mutant, whereas plasmid pGOB19, with *rbfA* in the opposite orientation, did not mediate suppression (Fig. 3). The suppression by pGOB18 was stronger when IPTG was added to the medium, which indicated that expression of *rbfA* from the *lac* promoter in the plasmid was responsible for the observed suppression. Further, these findings also imply that the suggested internal promoter for *rbfA* is not strong enough to mediate suppression. To see if there was any mutation in

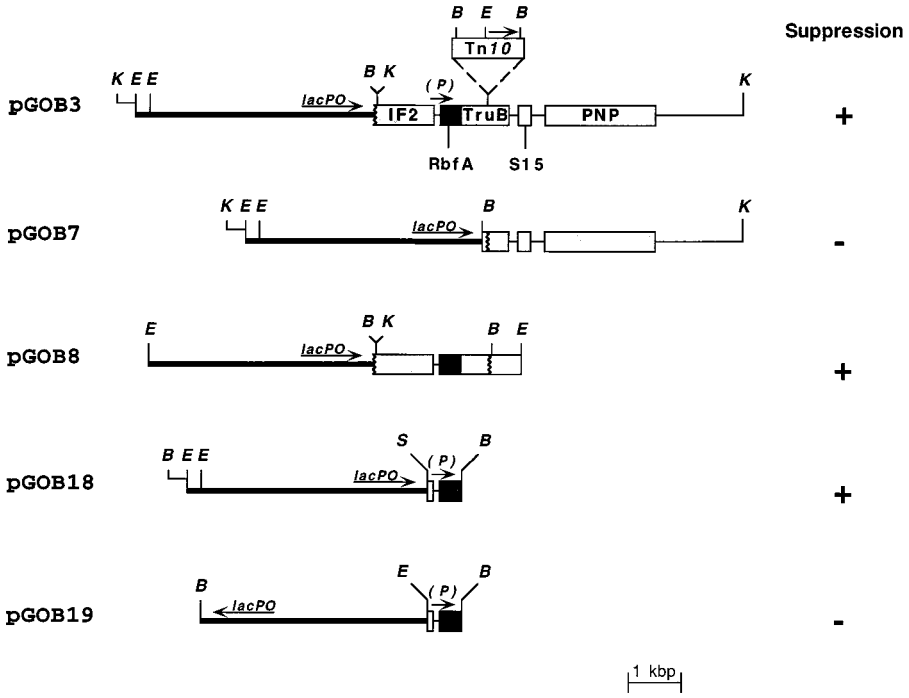


FIG. 3. Suppression of the slow growth of a Δ*rimM-2*-containing mutant by plasmids that carry different parts of the *nusA* operon. The suppression level was judged after single-cell outstreaks on rich-medium plates. Plasmid pGOB18 conferred stronger suppression in the presence of 0.25 mM IPTG than in the absence of IPTG. IF2, translational initiation factor IF2; TruB, tRNA Ψ55 synthase; PNP, polynucleotide phosphorylase. Restriction sites used in the plasmid constructions: *B*, *Bam*HI; *E*, *Eco*RI; *K*, *Kpn*I; *S*, *Sal*I. +, suppression; −, no suppression.

*rbfA* that could explain the observed suppression, the chromosomal region corresponding to the insert in pGOB18 was sequenced from *sdr-43* as well as *sdr*$^+$ strains after PCR amplification and cloning into pUC119. To our surprise, there was no mutation in that part of the chromosome. Therefore, we cloned the similar fragment from the wild-type strain MW100 into pCL1921 and found that the resulting plasmid, pGOB22, also suppressed the slow growth of the Δ*rimM-2* mutant in an IPTG-dependent manner (data not shown). These results strongly suggest that the suppression observed for the plasmid-containing strains was due to increased expression of the wild-type *rbfA* gene.

To see if any of the suppressor mutations other than *sdr-43* was linked to *rbfA*, the ability of the regions flanking *truB2422*::mini-Tn*10*Cm in the suppressor-free strain GOB113 to cross out the other suppressor mutations was examined. Phage P1 was grown on strain GOB113, and the different suppressor strains (PW093 to PW121) were transduced with the obtained lysate, selecting for Cm$^r$. The growth of the obtained transductants was examined by single-cell outstreaks on rich-medium plates. For 23 of the 29 strains tested, a majority of the transductants showed the slow-growth phenotype characteristic for the suppressor-free Δ*rimM-2* mutant, indicating that the regions containing the suppressor mutations had been replaced by the corresponding wild-type region from the donor strain. Thus, this result demonstrates that the suppressor mutations in 23 of the suppressor strains were tightly linked to *rbfA*.

**The suppressor mutation *sdr-43* increases the amount of *rbfA*-specific mRNA.** The observed multicopy suppression by *rbfA* implied that the chromosomally located mutation *sdr-43* of strain PW109 suppressed slow growth and translational deficiency by increasing expression of *rbfA*. Since there was no mutation in *rbfA* or in the 239 bp preceding *rbfA* in strain PW109, we reasoned that the suppressor mutation was not likely to have increased the translational efficiency of *rbfA* but would be a mutation increasing the synthesis or stability of the *rbfA* mRNA. Therefore, the amounts of *rbfA* mRNA in different strains were measured by Northern blot analysis using a probe corresponding to the *rbfA* gene (probe B in Fig. 4A). Evidently, strains PW109 (*sdr-43* Δ*rimM-2*) and GOB083 (*sdr-43 rimM*$^+$) had severalfold-increased levels of one *rbfA*-specific mRNA species of 2.6 to 3 kb (Fig. 4B). The size of this mRNA species was difficult to assess due to the proximity on the gels of the abundant 23S rRNA, which distorted the migration pattern. Similar results were obtained when a DNA fragment specific for the 3′ half of the *rbfA* gene was used as a probe (data not shown). Two mRNA species showed increased levels in the *sdr-43*-containing strains PW109 and GOB083 relative to those in the *sdr*$^+$ strains (Fig. 4C) when the mRNA was probed with a fragment corresponding to the region upstream from a transcriptional terminator preceding the *rbfA* gene (probe C in Fig. 4A). The size of the longer of these two mRNAs corresponded to that of the mRNA also detected with probe B, whereas the shorter mRNA (approximately 900 nucleotides [nt]) was specific for probe C. These findings suggest that both mRNAs have their 5′ ends within the *infB* gene preceding *rbfA* and that the longer mRNA covers the *rbfA* gene, while the shorter is the result of termination at the transcriptional terminator just upstream of *rbfA*. When the mRNA was probed with the region corresponding to *p15a*, the second gene of the *nusA* operon (probe D in Fig. 4A), two mRNA species of approximately 6.7 and 4.8 kb were detected (Fig. 4D). Note that the exposure times in Fig. 4B and C were shorter than that in Fig. 4D in order to avoid overexposure of the two bands corresponding to the mRNAs which had dra-

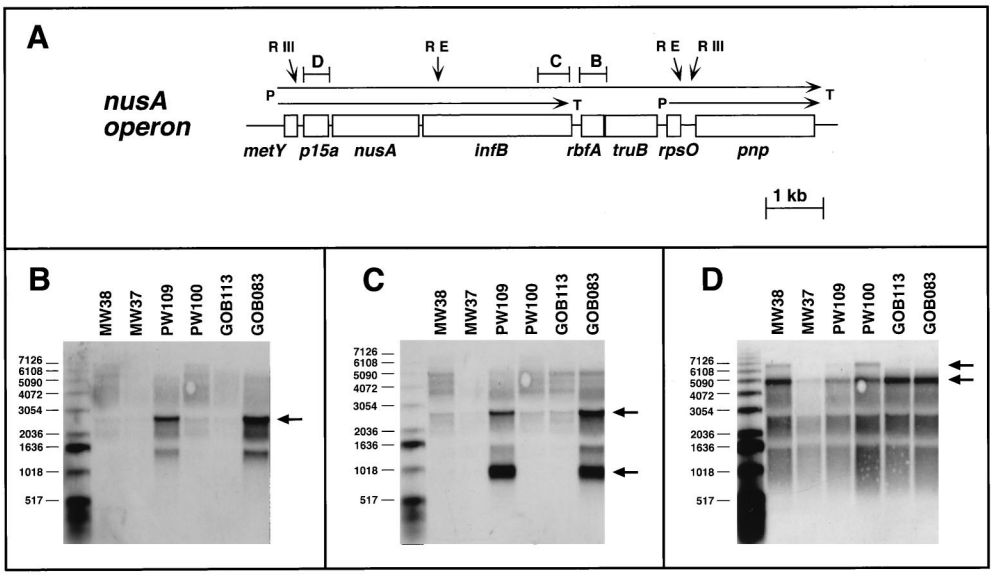


FIG. 4. Northern blot analysis of *nusA* operon mRNA. (A) Genetic organization of the *nusA* operon. Abbreviations: B, C, and D, probes used in the experiments for which results are shown in panels B, C, and D, respectively; R III and R E, processing sites for RNase III (34, 35) and RNase E (25, 36), respectively; (B through D) P, promoter; T, terminator. Five micrograms of total RNA was subjected to electrophoresis in an agarose gel containing formaldehyde, transferred to a Hybond N filter, and probed with a radiolabeled PCR fragment (probe D). The probe was removed by washing, and the filter was reprobed twice (probes C and B). The exposure times in the experiments for which results are shown in panels B and C were shorter than those in the experiment for which results are shown in panel D in order to avoid overexposure of the bands in strains PW109 and GOB083. The sizes of the $\gamma$-$^{32}$P-labeled ATP kinase-treated fragments of the 1-kb DNA ladder from GIBCO BRL Life Technologies Inc. (Gaithersburg, Md.) are indicated. The strains used (with the relevant genetic markers in parentheses) were MW38 (*rimM*$^+$), MW37 (Δ*rimM-2*), PW109 (Δ*rimM-2 sdr-43*), PW100 (Δ*rimM-2 sdr-34*), GOB113 (*rimM*$^+$ *sdr*$^+$), and GOB083 (*rimM*$^+$ *sdr-43*).

matically increased levels in strains PW109 and GOB083. With longer exposure times, the 4.8-kb mRNA was also detected with probe C, and the 6.7-kb mRNA was detected with both probes B and C (data not shown). Probably, both the 6.7- and the 4.8-kb mRNAs start at the RNase III processing site upstream of *p15a*. The apparent lengths of the mRNAs and the results with probes B and C suggest that the shorter mRNA terminates at the transcriptional terminator preceding *rbfA*, while the longer also contains the *rbfA* and *truB* genes. The amounts of the 6.7- and 4.8-kb mRNAs were not higher in strains containing *sdr-43* (PW109 and GOB083) than in the *sdr*$^+$ strains (Fig. 4D), indicating that *sdr-43* increased the amounts of only promoter-distal parts of the operon mRNA. Interestingly, strain PW100, which contains *sdr-34* (one of the other suppressor mutations that are tightly linked to the *rbfA* gene) showed higher levels of the 6.7-kb, and possibly also of the 4.8-kb, mRNA species than strain PW109 (Fig. 4D). These two strains have similar growth rates, so the comparison seems relevant, whereas a comparison to the other strains might be obscured by secondary effects caused by their growth rate differences. (Strain MW37 grows threefold slower and strains MW38, GOB083, and GOB113 grow twofold faster than PW100 and PW109.) The 6.7-kb transcript was not detected in strains GOB083 and GOB113 because the mini-Tn*10*Cm insertion in *truB* probably results in premature termination of transcription.

In summary, two mutations that increase the translational proficiency of the Δ*rimM-2* mutant MW37 and are tightly linked to the *rbfA* gene increase the amounts of *rbfA*-specific mRNA species. One of the mutations, *sdr-43*, increases the amount of a 2.6- to 3-kb mRNA that starts within *infB*, whereas the other mutation, *sdr-34*, increases the amount of a 6.7-kb mRNA that probably starts upstream of *p15a*. Since both an increased gene copy number of *rbfA* and an increased amount of its mRNA were found to suppress the slow growth and translational deficiency of the the Δ*rimM-2* mutant, it seems likely that increased synthesis of the RbfA protein was responsible for the suppression.

**The Δ*rimM-2* mutant MW37 has a normal level of the RbfA protein.** To distinguish between the possibility that the RimM protein was needed for the expression of *rbfA* and the possibility that increased expression of *rbfA* somehow compensated for the lack of the RimM protein, we decided to identify RbfA on 2D protein gels. Since RbfA is a cold shock protein (15), bacterial cultures were labeled with [$^{35}$S]methionine before or 30 min after a shift in temperature from 37 to 15°C, and prepared total protein extracts were separated on 2D gels. The levels of known cold shock-induced proteins, such as CspA, CspG, and H-NS, increased upon the shift to the lower temperature (Fig. 5). One protein spot that increased in intensity was putatively identified as RbfA based on a comparison of its position on our gels with that of a protein spot previously identified as RbfA (15). The protein spot was unambiguously identified as RbfA by addition of a [$^{35}$S]methionine-labeled minicell extract of a strain expressing *rbfA* from plasmid pGOB18 (Fig. 3) to a total protein extract of the *rbfA*Km$^r$ mutant GOB162 labeled after a shift from 37 to 15°C (Fig. 6). In strains MW38 (*rimM*$^+$) and MW37 (Δ*rimM-2*), the amount of RbfA at 37°C was below detection level; however, at 15°C, it seemed comparable in the two strains (compare Fig. 5B and 7C). In fact, the levels of RbfA relative to those of total protein were 0.56 and 0.45% in strains MW38 and MW37, respectively, as demonstrated by scanning and analysis of the autoradiographs shown (data not shown). This demonstrates that the RimM protein is not needed for the expression of *rbfA*. Moreover, in the suppressor strain PW109, the level of RbfA was severalfold higher than that in the suppressor-free strain MW37 at both 15 and 37°C (Fig. 7). The amount of RbfA at 15°C relative to that of total protein was found to be approximately sixfold higher in the suppressor strain PW109 than in

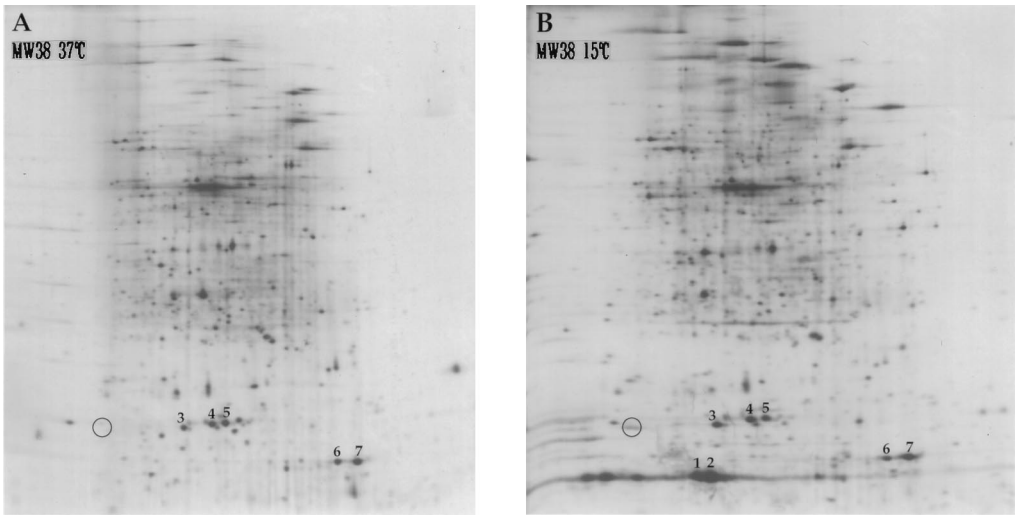


FIG. 5. Syntheses of individual proteins at 37°C and after a shift in temperature to 15°C. Total cell extracts of strain MW38 (*rimM*$^+$ *rbfA*$^+$) labeled with [$^{35}$S]methionine just prior to (A) and 30 min after (B) the shift to 15°C were separated on 2D gels. The indicated proteins are as follows (protein labels shown in parentheses): proteins CspG (1), CspA (2), and H-NS (3) and r-proteins S6 (4 and 5), L12 (6), and L7 (7). The identities of these proteins were obtained by comparing our gels with those of Fang et al. (11) and Jones and Inouye (14). A protein putatively identified as RbfA is indicated by a circle.

strain MW37 (data not shown). In conclusion, the translational deficiency and slow growth of the Δ*rimM-2* mutant MW37 do not result from reduced levels of RbfA; however, the observed suppression in strain PW109 results from overexpression of *rbfA*.

**The Δ*rimM-2* mutant MW37 is deficient in the processing of 16S rRNA.** RbfA has been shown to act as a multicopy suppressor of a mutation in the 5′-terminal helix of 16S rRNA, which causes cold sensitivity (10). RbfA has also been found associated with free 30S ribosomal subunits but not with 70S ribosomes and has been suggested to interact with the 5′-terminal helix of 16S rRNA during maturation of the 30S subunits (10). Therefore, we wanted to learn if the Δ*rimM-2* mutant MW37 had a defect in the maturation of 16S rRNA. Primer extension reactions were run on total RNA from different strains by using primers binding downstream from the 5′ ends of mature 5S, 16S, and 23S rRNA. In the *rimM*$^+$ strain MW38, most of the rRNA had 5′ ends corresponding to mature rRNA (Fig. 8). However, in the Δ*rimM-2* mutant MW37, approximately 50% of the 16S rRNA molecules had not been processed completely (Fig. 8; Table 3) and were found in a precursor form corresponding to the product of cutting at the RNase III site 115 nt upstream of the 5′ end of mature 16S rRNA. We examined if in addition, RbfA was required for proper processing of rRNA. Evidently, the *rbfA*::Km$^r$ mutant GOB162 showed the same dramatically elevated levels of the precursor form of 16S rRNA as did the Δ*rimM-2* mutant MW37 (Fig. 8; Table 3). Thus, both RimM and RbfA seem important for the maturation of 16S rRNA. However, the increased expression of *rbfA* in the suppressor strain PW109 seemed to increase the efficiency of processing of 16S rRNA only slightly (Fig. 8; Table 3).

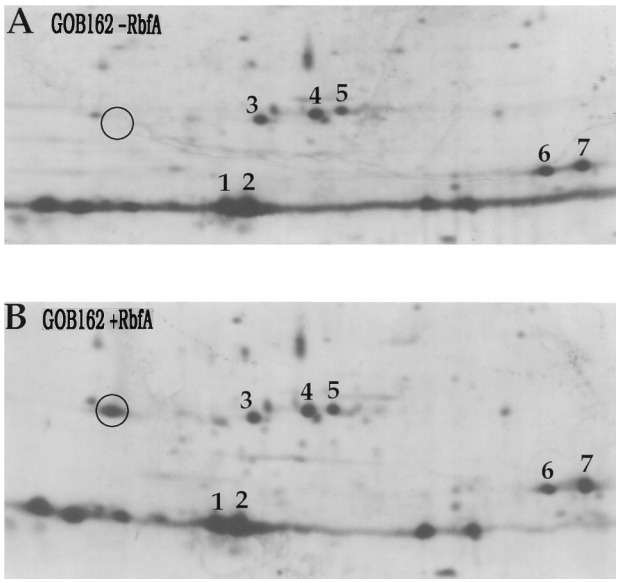


FIG. 6. Identification of RbfA on 2D gels. (A) A total cell extract of strain GOB162 (*rbfA*::Km$^r$) labeled with [$^{35}$S]methionine 30 min after a shift in temperature from 37 to 15°C was separated on 2D gels. (B) A [$^{35}$S]methionine-labeled minicell extract of strain AA10, expressing *rbfA* from plasmid pGOB18, was added to the total extract. The indicated proteins are as follows (protein labels shown in parentheses): proteins CspG (1), CspA (2), and H-NS (3) and r-proteins S6 (4 and 5), L12 (6), and L7 (7). The position of RbfA is indicated by a circle.

## DISCUSSION

In the present study we have isolated 29 fast-growing derivatives of a strain in which the *rimM* gene (formerly called *21K* and *yfjA*) of the *trmD* operon in *E. coli* has been deleted. Twenty-three of the suppressor mutations were shown to be linked to the *truB* gene of the *nusA* operon at 68.9 min on the chromosome. All the suppressor mutations that were tested partially suppressed the translational deficiency of the Δ*rimM* mutant. In the process of localizing one of these mutations, we discovered that an increased gene dosage of the wild-type *rbfA* gene (coding for the ribosome binding factor RbfA), which precedes *truB*, partly suppressed the slow growth of a Δ*rimM* mutant. In agreement with this observation, the amount of the RbfA protein in strain PW109, which contains the suppressor mutation *sdr-43*, was found to be higher than that in suppressor-free strains. The suppressor mutation seems to affect the transcription or stability of the *rbfA* mRNA, since strains con-

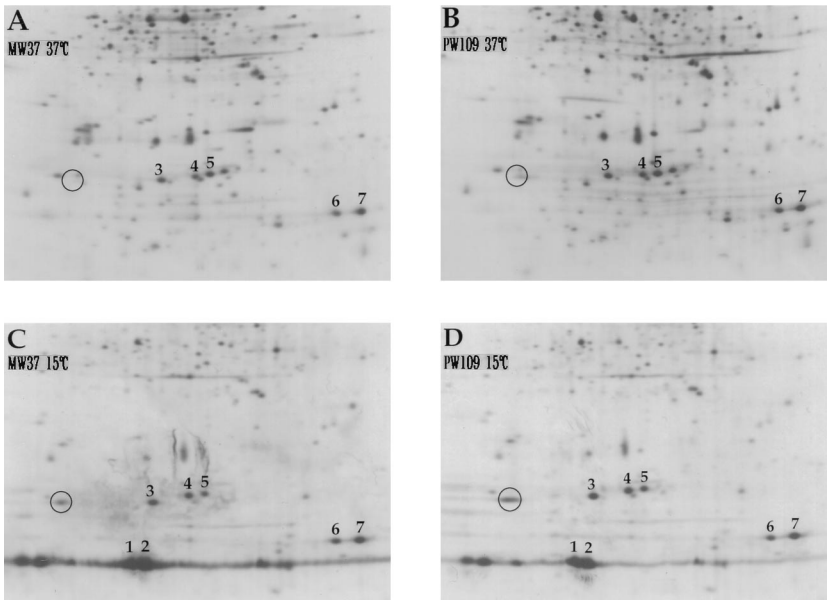


FIG. 7. Syntheses of individual proteins at 37°C and after a shift in temperature to 15°C. Strains MW37 (Δ*rimM-2*) and PW109 (Δ*rimM-2 sdr-43*) were labeled with [$^{35}$S]methionine just prior to and 30 min after the shift to 15°C. (A) MW37 at 37°C; (B) PW109 at 37°C; (C) MW37 at 15°C; (D) PW109 at 15°C. The indicated proteins are as follows (protein labels shown in parentheses): proteins CspG (1), CspA (2), and H-NS (3) and r-proteins S6 (4 and 5), L12 (6), and L7 (7). The position of RbfA is indicated by a circle.

taining the suppressor mutation had severalfold-increased levels of the *rbfA* mRNA. However, there was no mutation in the region covering the promoter for the entire operon, in the region containing a tentative internal promoter for *rbfA*, or in the *rbfA* structural gene. Moreover, there was no increased amount of the promoter-proximal part of the operon mRNA. The processing of the *nusA* operon is complex and has been only partly characterized (25, 35). The cleavage by RNase III downstream from *metY* releases the tRNA-Metf2 from the primary transcript and starts the decay of the downstream parts of the operon mRNA (35). Further, RNase E cleaves the *nusA* operon mRNA upstream of a hairpin structure at a site located at position +200 of the *infB* part of the mRNA (25). In a temperature-sensitive RNase E mutant, the *infB* mRNA accumulates at nonpermissive temperature, indicating that processing by RNase E accelerates the decay of the mRNA downstream of the cleavage site, including the part corresponding to the *rbfA* gene (25). At present, it is unclear whether the *sdr-43* mutation abolishes the processing at the RNase E site in *infB*, thereby increasing the stability of the *rbfA* part of the mRNA. However, at least the 900-nt mRNA species that had an increased level in *sdr-43*-containing strains (see Fig. 4C) was much too short to cover both the region hybridizing to the probe used and the region upstream of the RNase E site. Thus, if the *sdr-43* mutation abolishes the processing at the RNase E site, then some additional processing further downstream must have occurred to explain the size of at least the 900-nt mRNA species. Possibly, the *sdr-43* mutation alters the normal decay pathway of the *nusA* operon mRNA, resulting in the stabilization of the part of the mRNA corresponding to *rbfA*. In contrast, the other suppressor mutation, *sdr-34*, seems to have increased the synthesis or stability of a 6.7-kb transcript starting upstream of *p15a* and probably terminating downstream of *truB*.

The results of the measurements of the relative amounts of the precursor and mature forms of 16S rRNA in the different mutants seem contradictory. Both RimM and RbfA seem to be important for the processing of pre-16S rRNA, and an increased synthesis of RbfA suppresses the translational deficiency caused by the lack of the RimM protein. Therefore, one would expect the increased synthesis of RbfA to increase dramatically the ratio of mature 16S rRNA to the precursor form. However, the amount of mature 16S rRNA relative to the precursor form was only slightly higher in the RbfA-overproducing strain than in the Δ*rimM* mutant. Possibly, the absolute rate of rRNA synthesis in the suppressor strain is higher than that in the Δ*rimM* mutant, which implies that the absolute rate of production of mature 16S rRNA per unit of time would also be higher, allowing for a higher growth rate of the cells. Alternatively, increased synthesis of RbfA might improve the function of the ribosomes without affecting the processing of pre-16S rRNA.

RbfA has been shown to act as a high-copy-number suppressor of a cold-sensitive mutation in the 5′-terminal helix of 16S rRNA, and the growth of a strain lacking RbfA is cold sensitive (10). Recently, RbfA has been shown to be a cold shock protein (15). Strains that either have *rbfA* inactivated or contain the cold-sensitive mutation in the 5′-terminal helix of 16S rRNA show a constitutively induced cold shock response when shifted from 37 to 15°C and are unable to adapt their growth to the lower temperature (15). RbfA is associated with free 30S ribosomal subunits but not with 70S ribosomes and has been suggested to interact with the 5′-terminal helix region of 16S rRNA during a late step in maturation of the 30S subunits (10). Interestingly, the growth of Δ*rimM* mutants is slightly cold sensitive, and the RimM protein has affinity for the 30S ribosomal subunit (7); also, as demonstrated here, both RimM and RbfA seem to be important for the maturation of 16S rRNA. Evidently, increased expression of *rbfA* suppresses both a cold-sensitive mutation in 16S rRNA (10, 15) and the slow growth and translational deficiency of a Δ*rimM* mutant. It was proposed that the cold sensitivity caused by the mutation in the 5′-terminal helix of 16S rRNA results from the inability of RbfA to interact with the helix and that this deficiency is

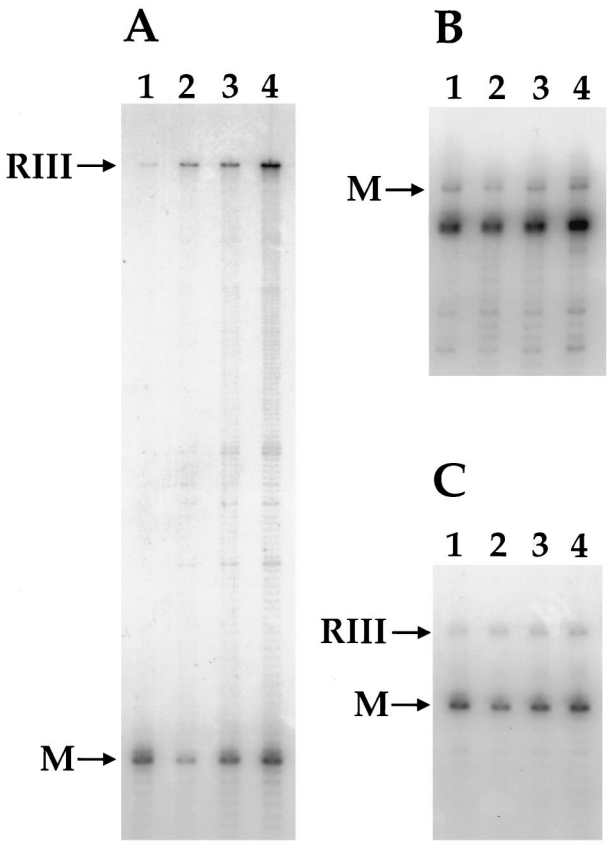


FIG. 8. Primer extension analysis of the 5′ ends of 5S, 16S, and 23S rRNA in wild-type and mutant strains. Lanes 1, strain MW38 (*rimM*$^+$ *rbfA*$^+$); lanes 2, strain MW37 (Δ*rimM-2 rbfA*$^+$); lanes 3, strain PW109 (Δ*rimM-2 sdr-43 rbfA*$^+$); lanes 4, strain GOB162 (*rimM*$^+$ *rbfA*::Km$^r$). The sizes of the primer extension products obtained were determined by comparing the mobilities with those of a known DNA sequencing ladder. (A) RIII indicates a primer extension product of 179 nt corresponding to pre-16S rRNA processed at the RNase III site 115 nt upstream of the 5′ end of mature 16S. M indicates a product of 64 nt corresponding to the 5′ end of mature 16S rRNA. (B) M indicates a primer extension product of 63 nt corresponding to mature 5S rRNA. (C) RIII indicates a primer extension product of 65 nt corresponding to pre-23S rRNA processed at the RNase III site 7 nt upstream of the 5′ end of mature 23S. M indicates a product of 58 nt corresponding to the 5′ end of mature 23S rRNA.

suppressed by increased expression of *rbfA* (10). We hypothesize that the reason why increased *rbfA* expression also suppresses the translational deficiency of the Δ*rimM* mutant is that in the absence of the RimM protein, RbfA might have a reduced ability to interact with the helix. However, the lack of the RimM protein has a much more profound effect than has the lack of the RbfA protein on the growth rate at 37°C (data not shown). Thus, the slow growth of a Δ*rimM* mutant cannot be attributed only to an inability of RbfA to interact with the ribosomal 30S subunits. This also explains why increased expression of *rbfA* only partially suppressed the lack of the RimM protein.

In the processing of rRNA, RNase III introduces a double cleavage in each of two stems that produce 17S and pre-23S rRNA (see reference 1a). The products formed are precursors that are further processed to complete the maturation process. In the case of the maturation of 16S rRNA, at least two enzymes are involved in the final processing steps. Since the *rimM* and *rbfA* mutants studied here both had increased levels of pre-16S rRNA produced by RNase III, RimM and RbfA might be two of these processing enzymes. However, neither of the two proteins seem responsible for the final processing step, since both the *rimM* and *rbfA* mutants produce mature 16S rRNA. Formally, the possibility exists that RimM and RbfA both possess the activity needed for the last processing step and that they can substitute for each other, since increased expression of *rbfA* suppressed the translational deficiency of the Δ*rimM* mutant. We find this explanation unlikely, since severalfold-increased expression of *rimM* from a plasmid could not suppress the slow growth of a *rbfA*::Km$^r$ mutant at 37°C, whereas it completely complemented the slow growth of a Δ*rimM* mutant (data not shown). In fact, the plasmid-mediated expression of *rimM* dramatically impaired the growth of the *rbfA*::Km$^r$ mutant (data not shown). Moreover, a *rimM rbfA* mutant grew slightly more slowly and formed colonies more heterogeneous in size on rich-medium plates than a Δ*rimM* mutant (data not shown). These findings suggest that the RimM and RbfA proteins have different functions in the cell, and they are consistent with a model in which the RimM protein is needed in a step prior to RbfA during the maturation of 16S rRNA.

The conversion of pre-16S rRNA produced by RNase III to mature 16S rRNA occurs within 30S subunits (see reference 29). It has been demonstrated that pre-16S rRNA is found only in 30S (or pre-30S) ribosomal subunits and not in 70S ribosomes both for wild-type cells (21, 22) and for 16S rRNA mutants with a reduced processing rate of pre-16S rRNA (41). Further, ribosomes containing pre-16S rRNA are inactive in translation, as demonstrated by reconstitution experiments (51). Thus, only after pre-16S rRNA has been processed to 16S rRNA can the 30S subunits participate in translation, probably because the secondary structure between the 5′ and 3′ ends of 16S rRNA within the pre-16S form is not present in the mature 30S subunits, where the 5′ and 3′ ends of 16S rRNA are far from each other (see reference 6). Thus, the reduced translational efficiency of the ribosomes in the Δ*rimM* mutant cannot be attributed to the 30S ribosomal subunits which contain pre-16S rRNA, since processing of pre-16S rRNA must precede function. This indicates that in the Δ*rimM* mutant, the ribosomes that contain mature 16S rRNA have a reduced function. Since correct 30S subunit assembly is a prerequisite for maturation of 16S rRNA, a deficiency in the assembly of the 30S subunits of the Δ*rimM* mutant might explain both a reduced function of ribosomes active in translation and a reduced efficiency in the processing of pre-16S rRNA. That the 30S subunits of Δ*rimM* mutants might be different from those in *rimM*$^+$ strains is supported by the finding that alterations in the region of r-protein S13 that binds 16S rRNA partly suppress the translational deficiency of a Δ*rimM* mutant (7).

We propose that RimM and RbfA are part of the 30S subunits prior to or during the final step in the processing of 16S rRNA, since both proteins have been found associated with free 30S ribosomal subunits (7, 10). The two proteins are not necessarily the actual processing enzymes but could be some accessory proteins needed for efficient assembly of the 30S subunits. In recent years a number of reports have indicated that nonribosomal proteins might facilitate the correct assembly of the ribosomal subunits. For example, it has been implied that the chaperone protein DnaK and two ATP-dependent RNA helicases assist in ribosome assembly: strains with temperature-sensitive mutations in *dnaK* are deficient in ribosome assembly at high temperatures (1), whereas overproduction of the RNA helicases SrmB and DeaD can suppress some mutations in the *rplX* gene, which encodes r-protein L24 (29a), and in the *rpsB* gene, which encodes r-protein S2 (43a), respectively. Possibly, RimM and RbfA assist some of the r-proteins

TABLE 3. Efficiency of 16S and 23S rRNA processing in different strains

| Strain | Amt of rRNA[a] | | | | | | | | | | | |
|---|---|---|---|---|---|---|---|---|---|---|---|---|
| | 16S | | | | | | 23S | | | | | |
| | RIII ($10^6$ cpm[b]) | | M ($10^6$ cpm[b]) | | M/(RIII + M) | | RIII ($10^6$ cpm[b]) | | M ($10^6$ cpm[b]) | | M/(RIII + M) | |
| | Expt I | Expt II | Expt I | Expt II | Expt I | Expt II | Expt I | Expt II | Expt I | Expt II | Expt I | Expt II |
| MW38 (*rimM*$^+$) | 0.046 | 0.65 | 2.7 | 8.5 | **0.98** | **0.93** | 0.12 | 0.79 | 5.0 | 11.2 | 0.98 | 0.93 |
| MW37 (Δ*rimM-2*) | 0.46 | 2.9 | 0.79 | 2.2 | **0.63** | **0.43** | 0.18 | 3.6 | 2.3 | 7.4 | 0.93 | 0.67 |
| PW109 (Δ*rimM-2 sdr-43*) | 0.68 | 7.9 | 2.0 | 9.4 | **0.74** | **0.54** | 0.25 | 1.5 | 4.5 | 10.5 | 0.95 | 0.87 |
| GOB162 (*rbfA*::Km$^r$) | 3.0 | ND | 3.6 | ND | **0.54** | | 0.38 | ND | 6.0 | ND | 0.94 | |

[a] The amount of rRNA was determined by primer extension as described in Materials and Methods.
[b] The amounts of radioactivity in the primer extension products were quantified with a PhosphorImager from Molecular Dynamics, Inc. See also the legend to Fig. 8. ND, not determined.

in their binding to 16S rRNA. Alternatively, the two proteins might stabilize RNA secondary structures needed for correct processing or help to refold the mature 16S rRNA after processing has been completed. In fact, since RbfA has been suggested to bind to the 5′-terminal helix of mature 16S rRNA, it might be involved in the formation of that structure. Also, the RimM protein might bind to 16S rRNA, since two different RNA binding motifs are present in the protein (7).

Experiments are in progress to elucidate what role the RimM protein plays in the maturation of 16S rRNA and the 30S ribosomal subunits and what the relation is between RimM and RbfA in those processes.

## ACKNOWLEDGMENTS

Glenn Björk and Britt Persson are gratefully acknowledged for stimulating and fruitful discussions.

P.M.W. was supported by the Swedish Natural Science Research Council (B-BU 9911) and by the Magnus Bergvalls Stiftelse.

## REFERENCES

1. **Alix, J.-H., and M.-F. Guérin.** 1993. Mutant DnaK chaperones cause ribosome assembly defects in *Escherichia coli*. Proc. Natl. Acad. Sci. USA **90:** 9725–9729.
1a. **Apirion, D., and A. Miczak.** 1993. RNA processing in prokaryotic cells. Bioessays **15:**113–120.
2. **Bertani, G.** 1951. Studies on lysogenesis. I. The mode of phage liberation by lysogenic *Escherichia coli*. J. Bacteriol. **62:**293–300.
3. **Björk, G. R.** 1987. Modification of stable RNA, p. 719–731. *In* F. C. Neidhardt, J. L. Ingraham, K. B. Low, B. Magasanik, M. Schaechter, and H. E. Umbarger (ed.), *Escherichia coli* and *Salmonella typhimurium*: cellular and molecular biology, vol. 2. American Society for Microbiology, Washington, D.C.
4. **Björk, G. R., J. U. Ericson, C. E. Gustafsson, T. G. Hagervall, Y. H. Jönsson, and P. M. Wikström.** 1987. Transfer RNA modification. Annu. Rev. Biochem. **56:**263–287.
5. **Björk, G. R., P. M. Wikström, and A. S. Byström.** 1989. Prevention of translational frameshifting by the modified nucleoside 1-methylguanosine. Science **244:**986–989.
6. **Brimacombe, R., and W. Stiege.** 1985. Structure and function of ribosomal RNA. Biochem. J. **229:**1–17.
7. **Bylund, G. O., B. C. Persson, L. A. C. Lundberg, and P. M. Wikström.** 1997. A novel ribosome-associated protein is important for efficient translation in *Escherichia coli*. J. Bacteriol. **179:**4567–4574.
8. **Byström, A. S., K. J. Hjalmarsson, P. M. Wikström, and G. R. Björk.** 1983. The nucleotide sequence of an *Escherichia coli* operon containing genes for the tRNA($m^1$G)methyltransferase, the ribosomal proteins S16 and L19 and a 21-K polypeptide. EMBO J. **2:**899–905.
9. **Byström, A. S., A. von Gabain, and G. R. Björk.** 1989. Differentially expressed *trmD* ribosomal protein operon of *Escherichia coli* is transcribed as a single polycistronic mRNA species. J. Mol. Biol. **208:**575–586.
10. **Dammel, C. S., and H. F. Noller.** 1995. Suppression of a cold-sensitive mutation in 16S rRNA by overexpression of a novel ribosome-binding factor, RbfA. Genes Dev. **9:**626–637.
11. **Fang, L., W. Jiang, W. Bae, and M. Inouye.** 1997. Promoter-independent cold-shock induction of *cspA* and its derepression at 37°C by mRNA stabilization. Mol. Microbiol. **23:**355–364.
12. **Hagervall, T. G., T. M. Tuohy, J. F. Atkins, and G. R. Björk.** 1993. Deficiency of 1-methylguanosine in tRNA from *Salmonella typhimurium* induces frameshifting by quadruplet translocation. J. Mol. Biol. **232:**756–765.
13. **Held, W. A., and M. Nomura.** 1975. *Escherichia coli* 30S ribosomal proteins uniquely required for assembly. J. Biol. Chem. **250:**3179–3184.
14. **Jones, P. G., and M. Inouye.** 1994. The cold-shock response—a hot topic. Mol. Microbiol. **11:**811–818.
15. **Jones, P. G., and M. Inouye.** 1996. RbfA, a 30S ribosomal binding factor, is a cold-shock protein whose absence triggers the cold-shock response. Mol. Microbiol. **21:**1207–1218.
16. **Kennedy, N., L. Beutin, M. Achtman, R. Skurray, U. Rahmsdorf, and P. Herrlich.** 1977. Conjugation proteins encoded by the F sex factor. Nature **270:**580–585.
17. **Kleckner, N., J. Bender, and S. Gottesman.** 1991. Uses of transposons with emphasis on Tn*10*. Methods Enzymol. **204:**139–180.
18. **Kohara, Y., K. Akiyama, and K. Isono.** 1987. The physical map of the whole *E. coli* chromosome: application of a new strategy for rapid analysis and sorting of a large genomic library. Cell **50:**495–508.
19. **Kulakauskas, S., P. M. Wikström, and D. E. Berg.** 1991. Efficient introduction of cloned mutant alleles into the *Escherichia coli* chromosome. J. Bacteriol. **173:**2633–2638.
20. **Lerner, C. G., and M. Inouye.** 1990. Low copy number plasmids for regulated low-level expression of cloned genes in *Escherichia coli* with blue/white insert screening capability. Nucleic Acids Res. **18:**4631.
21. **Lindahl, L.** 1973. Two new ribosomal precursor particles in *E. coli*. Nature New Biol. **243:**170–172.
22. **Lindahl, L.** 1975. Intermediates and time kinetics of the in vivo assembly of *Escherichia coli* ribosomes. J. Mol. Biol. **92:**15–37.
23. **Médigue, C., A. Viari, A. Hénaut, and A. Danchin.** 1991. *Escherichia coli* molecular genetic map (1500 kbp): update II. Mol. Microbiol. **5:**2629–2640.
24. **Miller, J. H.** 1972. Experiments in molecular genetics. Cold Spring Harbor Laboratory, Cold Spring Harbor, N.Y.
25. **Mortensen, K. K., E. Hajnsdorf, P. Régnier, and H. U. Sperling Petersen.** 1995. Improved recombinant tandem expression of translation initiation factor IF2 in RNase E deficient *E. coli* cells. Biochem. Biophys. Res. Commun. **214:**1254–1259.
26. **Mullis, K. B., and F. A. Faloona.** 1987. Specific synthesis of DNA *in vitro* via a polymerase-catalyzed chain reaction. Methods Enzymol. **155:**335–350.
27. **Neidhardt, F. C., P. L. Bloch, S. Pedersen, and S. Reeh.** 1977. Chemical measurement of steady-state levels of ten aminoacyl-transfer ribonucleic acid synthetases in *Escherichia coli*. J. Bacteriol. **129:**378–387.
28. **Neidhardt, F. C., P. L. Bloch, and D. F. Smith.** 1974. Culture medium for enterobacteria. J. Bacteriol. **119:**736–747.
29. **Nierhaus, K. H.** 1991. The assembly of prokaryotic ribosomes. Biochimie **73:**739–755.
29a. **Nishi, K., F. Morel-Deville, J. W. B. Hershey, T. Leighton, and J. Schnier.** 1988. An eIF-4A-like protein is a suppressor of an *Escherichia coli* mutant defective in 50S ribosomal subunit assembly. Nature **336:**496–498.
30. **Oberto, J., E. Bonnefoy, E. Mouray, O. Pellegrini, P. M. Wikström, and J. Rouvière-Yaniv.** 1996. The *Escherichia coli* ribosomal protein S16 is an endonuclease. Mol. Microbiol. **19:**1319–1330.
31. **O'Farrell, P. H.** 1975. High resolution two-dimensional electrophoresis of proteins. J. Biol. Chem. **250:**4007–4021.
32. **Orndorff, P. E., P. A. Spears, D. Schauer, and S. Falkow.** 1985. Two modes of control of *piA*, the gene encoding type 1 pilin in *Escherichia coli*. J. Bacteriol. **164:**321–330.
33. **Persson, B. C., G. O. Bylund, D. E. Berg, and P. M. Wikström.** 1995. Functional analysis of the *ffh-trmD* region of the *Escherichia coli* chromosome by using reverse genetics. J. Bacteriol. **177:**5554–5560.
34. **Portier, C., L. Dondon, M. Grunberg Manago, and P. Régnier.** 1987. The first step in the functional inactivation of the *Escherichia coli* polynucleotide

phosphorylase messenger is a ribonuclease III processing at the 5′ end. EMBO J. **6:**2165–2170.
35. **Régnier, P., and M. Grunberg Manago.** 1989. Cleavage by RNase III in the transcripts of the *metY-nusA-infB* operon of *Escherichia coli* releases the tRNA and initiates the decay of the downstream mRNA. J. Mol. Biol. **210:**293–302.
36. **Régnier, P., and E. Hajnsdorf.** 1991. Decay of mRNA encoding ribosomal protein S15 of *Escherichia coli* is initiated by an RNase E-dependent endonucleolytic cleavage that removes the 3′ stabilizing stem and loop structure. J. Mol. Biol. **217:**283–292.
37. **Saiki, R. K., S. Scharf, F. Faloona, K. B. Mullis, G. T. Horn, H. A. Erlich, and N. Arnheim.** 1985. Enzymatic amplification of β-globin genomic sequences and restriction site analysis for diagnosis of sickle cell anemia. Science **230:**1350–1354.
38. **Sambrook, J., E. F. Fritsch, and T. Maniatis.** 1989. Molecular cloning: a laboratory manual, 2nd ed. Cold Spring Harbor Laboratory Press, Cold Spring Harbor, N.Y.
39. **Sands, J. F., P. Régnier, H. S. Cummings, M. Grunberg Manago, and J. W. Hershey.** 1988. The existence of two genes between *infB* and *rpsO* in the *Escherichia coli* genome: DNA sequencing and S1 nuclease mapping. Nucleic Acids Res. **16:**10803–10816.
40. **Schleif, R., W. Hess, S. Finkelstein, and D. Ellis.** 1973. Induction kinetics of the L-arabinose operon of *Escherichia coli*. J. Bacteriol. **115:**9–14.
41. **Stark, M. J., R. J. Gregory, R. L. Gourse, D. L. Thurlow, C. Zwieb, R. A. Zimmermann, and A. E. Dahlberg.** 1984. Effects of site-directed mutations in the central domain of 16 S ribosomal RNA upon ribosomal protein binding, RNA processing and 30 S subunit assembly. J. Mol. Biol. **178:**303–322.
42. **Stöffler, G., M. Noah, M. Stöffler-Meilicke, and E. R. Dabbs.** 1984. The localization of protein L19 on the surface of 50S subunits of *Escherichia coli* aided by the use of mutants lacking protein L19. J. Biol. Chem. **259:**4521–4526.
43. **Thompson, R., and M. Achtman.** 1978. The control region of the F sex factor DNA transfer cistrons: restriction mapping and DNA cloning. Mol. Gen. Genet. **165:**295–304.
43a. **Toone, W. M., K. E. Rudd, and J. D. Friesen.** 1991. *deaD*, a new *Escherichia coli* gene encoding a presumed ATP-dependent RNA helicase, can suppress a mutation in *rpsB*, the gene encoding ribosomal protein S2. J. Bacteriol. **173:**3291–3302.
44. **VanBogelen, R. A., and F. C. Neidhardt.** 1990. Ribosomes as sensors of heat and cold shock in *Escherichia coli*. Proc. Natl. Acad. Sci. USA **87:**5589–5593.
45. **Vogel, H. J., and D. M. Bonner.** 1956. Acetylornithinase of *Escherichia coli*: partial purification and some properties. J. Biol. Chem. **218:**97–106.
46. **von Gabain, A., J. G. Belasco, J. L. Schottel, A. C. Chang, and S. N. Cohen.** 1983. Decay of mRNA in *Escherichia coli*: investigation of the fate of specific segments of transcripts. Proc. Natl. Acad. Sci. USA **80:**653–657.
47. **Wikström, P. M., and G. R. Björk.** 1988. Noncoordinate translation-level regulation of ribosomal and nonribosomal protein genes in the *Escherichia coli trmD* operon. J. Bacteriol. **170:**3025–3031.
48. **Wikström, P. M., and G. R. Björk.** 1989. A regulatory element within a gene of a ribosomal protein operon of *Escherichia coli* negatively controls expression by decreasing the translational efficiency. Mol. Gen. Genet. **219:**381–389.
49. **Wikström, P. M., A. S. Byström, and G. R. Björk.** 1988. Non-autogenous control of ribosomal protein synthesis from the *trmD* operon in *Escherichia coli*. J. Mol. Biol. **203:**141–152.
50. **Wikström, P. M., L. K. Lind, D. E. Berg, and G. R. Björk.** 1992. Importance of mRNA folding and start codon accessibility in the expression of genes in a ribosomal protein operon of *Escherichia coli*. J. Mol. Biol. **224:**949–966.
51. **Wireman, J. W., and P. S. Sypherd.** 1974. *In vitro* assembly of 30S ribosomal particles from precursor 16S RNA of *Escherichia coli*. Nature **247:**552–554.